

Two Approaches to Kinematics Modeling of Articulated Rovers¹

Mahmoud Tarokh, Lorena Mireles and Gregory McDermott

*Department of Computer Science
San Diego State University
San Diego, CA 92182-7720*

Abstract – This research report compares two approaches to kinematics modeling of articulated rovers with active suspension systems. The first method is based on taking the derivative of transformation matrices of various frame, and equating it with those of a general body in motion to obtain the Jacobian matrix of the rover. The second method is based on position and orientation velocity propagation through different frames. The methods are applied to an articulated rover similar to the JPL Sample Return rover. While both methods provide identical results, the second method is shown to be more straightforward and suitable for direct computer implementation.

1. Introduction

Articulated rovers are used increasingly in diverse applications such as terrestrial and planetary explorations [1]-[2], forestry [3], agriculture [4] mining industries [5], defense applications and hazardous material handling and demining [6]. Rovers with active suspension mechanisms [7] are capable of modifying their configurations by adjusting their suspension linkages and joints so as to change their center of mass, thus avoiding tipover while traversing rough and sloppy terrain.

Most research efforts on kinematics have concentrated on simple car-like four-wheel mobile robots moving on flat terrain, which we will refer to as ordinary mobile robots (OMRs). The kinematics modeling of these robots can be classified into two main approaches – geometric and transformation. The geometric approach [8]-[9] is intuitive but restrictive if used on its own. The transformation approach is widely employed by researchers and consists of a series of transformations, and their derivative to relate the motion of the wheels to the motion of the robot. One of the fundamental contributions using this approach is by Muir and Newman [10]. In this work, a matrix coordinate transformation algebra is developed to derive the equations of the motion of OMRs. Due to the underlying assumptions, this and similar approaches are only applicable to motion in 2-dimensional space, i.e. translation in the x-y plane and yaw rotation. They also assume perfect rolling motion on a flat, smooth surface with no side or rolling slip, and no motion along the z-axis, and thus the results are not applicable to articulated rovers (ATRs).

A number of other researchers have dealt with different aspects of OMR kinematics [11]-[13]. For example, Campion, et al [12] present a technique to classify OMRs for the study of the kinematics and dynamics models while taking into consideration the mobility restriction due to various constraints. The paper by Borestein [13] discusses kinematics of several connected OMRs with compliant linkage. Rajagopalan [14] uses a transformation approach to develop the kinematic model of OMRs with inclined steering column, and different combination of driving and steering wheels. The forward kinematics of a specific OMR with omni-directional wheels is derived in

¹ Section 2 of this report was published in M. Tarokh and G. McDermott, “Kinematics Modeling and Analysis of Articulated Rovers,” IEEE Trans. Robotics, vol. 21, No. 4, pp. 539-554, August 2005. Section 3 is part of a paper by G. McDermott, M. Tarokh and L. Mireles has been submitted to 7th IFAC Int. Conference on Robot Control, to be held in Italy, September 2006. Other sections have not been reported elsewhere.

[15], and the singularity configurations are identified. Williams et al [16] develop a dynamic model for omnidirectional robots that incorporates a wheel slip model. Tarokh et al [17] study the kinematics of a particular high mobility rover. Iagnemma and Dubowsky [18] propose a Kalman filter approach to estimate the rover wheel-ground contact angle for traction control. Balaram [19] employs a simple kinematics model and a state observer to estimate position, orientation, velocities and contact angles of a rover.

Rovers with adjustable suspension system have been considered by Sreenivasan and Waldron [20] for a specific vehicle. More recently, Iagnemma and Dubowsky [7] presented stability-based suspension control for a specific rover using an essentially geometric approach and performing a rather complex optimization procedure.

Despite these efforts, only recently a comprehensive kinematics model of an articulated rover was developed by Tarokh and McDermott [21] and McDermott, Tarokh and Mireles [22]. The goal of this report is to compare two approaches to kinematics modeling of articulated rovers with active suspension systems.

2. Method 1 – Modeling using Transformation Derivatives

In this section, we develop a general approach to kinematics modeling of an articulated rover. The emphasis here is on deriving the equations of motion of the rover components relative to a rover reference frame. We define an ATR as a wheeled mobile robot consisting of a main body connected to wheels via a set of linkages and joints. The rover is capable of locomotion over uneven terrain by rolling of the wheels and adjusting its joints, and the only contact with the terrain is at the wheel surfaces.

Fig. 1 illustrates the geometric definition of a general ATR. At any time t , the rover has an *instantaneous coordinate frame* R attached to its body that moves with the rover and is defined relative to a fixed, world coordinate frame. The rover configuration vector $u = [x_r \ y_r \ z_r \ \alpha_r \ \beta_r \ \gamma_r]^T$ is defined relative to the world coordinate frame W , where (x_r, y_r, z_r) is the position and $(\alpha_r, \beta_r, \gamma_r)$ is the orientation with heading α_r , pitch β_r and roll γ_r . Quantities of heading α_r , pitch β_r and roll γ_r in Fig. 1, are with respect to the instantaneous rover frame R . Each rover wheel also has an instantaneous coordinate frame A_i , $i = 1, 2, \dots, n$, attached to the wheel axle and defined relative to the rover body coordinate frame R , where n is the number of the wheels. The transformation between the rover coordinate frame R and each wheel axle coordinate frame A_i , denoted by the homogeneous transformation $T_{R,A_i}(q)$, depends on the specific rover linkages and joints represented here by the $v_q \times 1$ joint variable vector q . The dashed line in Fig. 1(b) represents any set of links and joints that exist between these two frames including the steering mechanism.

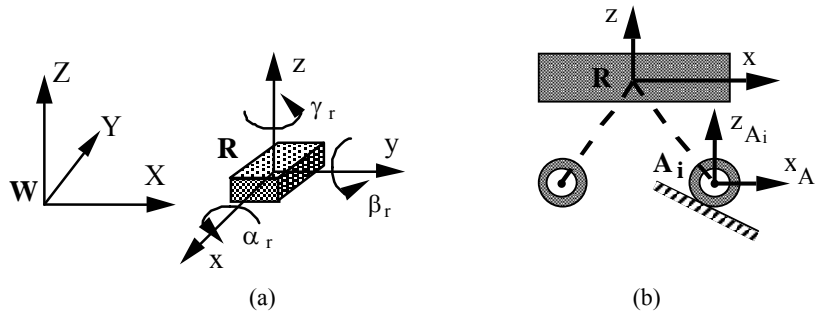


Fig. 1. Geometric description of a generalized ATR, (a) Perspective view. (b) Side view

In our analysis, each wheel is assumed to be represented by a rigid disc with a single point of contact with the terrain surface. Allowing multiple contact angles for each wheel makes the kinematics analysis extremely complex. A coordinate frame C_i , $i = 1, \dots, n$ is defined at each wheel's contact point as illustrated in Fig. 2, where its x -axis is tangent to the terrain at the point of contact and its z -axis is normal to the terrain. The contact angle δ_i is the angle between the z -axes of the i -th wheel axle and contact coordinate frames as shown in Fig. 2. This contact angle is a

key distinction between an OMR moving on flat surfaces and an ATR traversing uneven terrain. In the former case, the z-axis of the contact frame is aligned with the z-axis of the wheel axle and the contact angle is always zero whereas in the latter case δ_i is variable. The contact angles play an important role in the kinematics of ATRs.

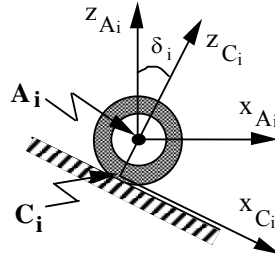


Fig. 2. Coordinate frames for terrain contact at wheel i .

The contact coordinate frame C_i is obtained from the axle coordinate frame A_i by rotating δ_i about the axle, then translating by the wheel radius r in the negative z direction. The corresponding transformation matrix from the axle A_i to contact C_i denoted by T_{A_i, C_i} is given by

$$T_{A_i, C_i}(\delta_i) = \begin{bmatrix} c\delta_i & 0 & s\delta_i & -r s\delta_i \\ 0 & 1 & 0 & 0 \\ -s\delta_i & 0 & c\delta_i & -r c\delta_i \\ 0 & 0 & 0 & 1 \end{bmatrix} \quad (1)$$

where $i=1,2,\dots, n$, and s and c denote sine and cosine. The transformation from the rover reference frame to wheel contact frame C_i is thus $T_{R, C_i}(q, \delta_i) = T_{R, A_i}(q) T_{A_i, C_i}(\delta_i)$. However, this transformation does not include rolling or slip, and thus does not reflect motion. In order to include motion, we consider the instantaneous contact frames $C_i(t - \Delta t)$ and $C_i(t)$, where Δt is a time increment as shown in Fig. 3.

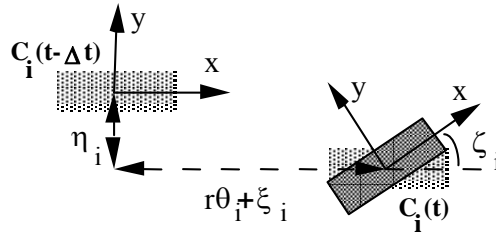


Fig. 3. Incremental motion by rolling and slip.

The wheel motion from $C_i(t - \Delta t) \equiv \bar{C}_i$ to $C_i(t) \equiv C_i$ is defined by a coordinate transformation corresponding to a wheel rolling translation $(r\theta_i + \xi_i)$ along the x-axis, where θ_i is the angular rotation and ξ_i is the rolling slip, a wheel side slip translation η_i along the y-axis, and a turn slip rotation ζ_i about the z-axis. Thus

$$T_{\bar{C}_i, C_i} = \begin{bmatrix} c\zeta_i & -s\zeta_i & 0 & r\theta_i + \xi_i \\ s\zeta_i & c\zeta_i & 0 & \eta_i \\ 0 & 0 & 1 & 0 \\ 0 & 0 & 0 & 1 \end{bmatrix} \quad (2)$$

Note that the z component of the translation motion is zero since no movement along the z -axis is allowed due to the fact that jumping of the wheel off the terrain or penetration of the wheel into the terrain is assumed not to occur.

The transformation from a wheel contact frame at time $t - \Delta t$ denoted by \bar{C}_i , to the rover frame R is

$$T_{\bar{C}_i,R} = T_{\bar{C}_i,C_i}(\theta_i, \varepsilon_i) T_{C_i,A_i}(\delta_i) T_{A_i,R}(q) \quad (3)$$

where $\varepsilon_i = [\xi_i \ \zeta_i \ \eta_i]^T$ is the slip vector, $T_{C_i,A_i}(\delta_i) = (T_{A_i,C_i}(\delta_i))^{-1}$, $T_{A_i,R}(q) = (T_{R,A_i}(q))^{-1}$, and the dependencies of the transformation matrices are shown with quantities inside the brackets.

To quantify the motion, we must relate changes in the rover configuration rate vector $\dot{u} = [\dot{x}_r \ \dot{y}_r \ \dot{z}_r \ \dot{\alpha}_x \ \dot{\beta}_y \ \dot{\gamma}_z]^T$ to the rover joint angle rates \dot{q} , wheel roll rates $\dot{\theta}_i$, and wheel slip rate vector $\dot{\varepsilon}_i$. To do this, we consider the matrix $T_{\bar{R},R}$ that describes the transformation from the rover frame at time $t - \Delta t$ to the rover frame at time t , which can be written as $T_{\bar{R},R} = T_{\bar{R},\bar{C}_i} T_{\bar{C}_i,R}$. Since $T_{\bar{R},\bar{C}_i}$ is independent of time, the derivative of $T_{\bar{R},R}$ is

$$\dot{T}_{\bar{R},R} = T_{\bar{R},\bar{C}_i} \dot{T}_{\bar{C}_i,R} \quad (4)$$

The transformation derivative $\dot{T}_{\bar{C}_i,R}$ defines the motion of the rover reference frame R relative to the wheel i coordinate frame \bar{C}_i . For a specific rover, $T_{\bar{C}_i,R}$ exists as given by (3) and its derivative can be computed as

$$\dot{T}_{\bar{C}_i,R} = \frac{\partial T_{\bar{C}_i,R}}{\partial q} \dot{q} + \frac{\partial T_{\bar{C}_i,R}}{\partial \theta_i} \dot{\theta}_i + \frac{\partial T_{\bar{C}_i,R}}{\partial \varepsilon_i} \dot{\varepsilon}_i + \frac{\partial T_{\bar{C}_i,R}}{\partial \delta_i} \dot{\delta}_i \quad (5)$$

We evaluate the partial derivatives in (5) at the reference condition. Now, $\dot{T}_{\bar{R},R}$ can also be found for a general body in motion using the position and orientation rates as [21]

$$\dot{T}_{\bar{R},R} = \begin{bmatrix} 0 & -\dot{\gamma}_r & \dot{\beta}_r & \dot{x}_r \\ \dot{\gamma}_r & 0 & -\dot{\alpha}_r & \dot{y}_r \\ -\dot{\beta}_r & \dot{\alpha}_r & 0 & \dot{z}_r \\ 0 & 0 & 0 & 1 \end{bmatrix} \quad (6)$$

Note that $\dot{T}_{\bar{R},R}$ is a skew symmetric matrix and the transformation product matrix on the right hand side of (4) also has the structure of (6). Substituting (5) and (6) into (4), evaluating the matrix product, and equating the like matrix elements on both sides of the resulting equation, we can determine rover configuration rate vector \dot{u} in terms of the joint angular rates vector \dot{q} , contact angle rate $\dot{\delta}_i$, wheel rolling rate $\dot{\theta}_i$, and wheel slip rate vector $\dot{\varepsilon}_i$.

Furthermore, these equations are linear in the time-derivatives \dot{q} , $\dot{\theta}_i$, $\dot{\delta}_i$, $\dot{\varepsilon}_i$ as seen from (5). These lead to an equation of the form

$$[\dot{x}_r \ \dot{y}_r \ \dot{z}_r \ \dot{\alpha}_r \ \dot{\beta}_r \ \dot{\gamma}_r]^T = J_i [\dot{q} \ \dot{\theta}_i \ \dot{\varepsilon}_i \ \dot{\delta}_i]^T \quad (7)$$

where J_i is the $6 \times (v_q + 5)$ wheel Jacobian matrix and v_q is dimension of the joint vector q . Equation (7) describes the contribution of individual wheel motion and the connecting joints to the rover body motion. The net body motion is the composite effect of all wheels and can be obtained by combining (7) into a single matrix equation as

$$\begin{bmatrix} I_6 \\ \vdots \\ I_6 \end{bmatrix} \begin{bmatrix} \dot{x}_r \\ \dot{y}_r \\ \dot{z}_r \\ \dot{\alpha}_r \\ \dot{\beta}_r \\ \dot{\gamma}_r \end{bmatrix} = J \begin{bmatrix} \dot{q} \\ \dot{\theta} \\ \dot{\varepsilon} \\ \dot{\delta} \end{bmatrix}; \quad \text{or} \quad E \dot{u} = J \dot{p} \quad (8)$$

where E is a $6n \times 6$ matrix that is obtained by stacking n 6×6 identity matrices, \dot{q} is the $v_q \times 1$ vector of rover joint angles, $\dot{\theta}$ is the $n \times 1$ vector of wheel rolling rates, $\dot{\varepsilon}$ is the $3n \times 1$ vector consisting of rolling $\dot{\xi}$, turn $\dot{\zeta}$ and side $\dot{\eta}$ slip rates, and $\dot{\delta}$ is the $n \times 1$ vector of contact angle rates. The rover Jacobian matrix J is a $6n \times (v_q + 5n)$ matrix formed from the individual wheel Jacobian matrices J_i , $i = 1, 2, \dots, n$ and \dot{p} is the $(v_q + 5n) \times 1$ vector of composite angular rates. Observe from (7) and (8), that J is a sparse matrix.

3. Method 2 – Modeling using Position/Orientation Velocity Propagation

In this method, we attach, as before, a number of frames starting from the wheel-terrain contact frame then going through the steering and suspension frames and finally to the rover reference frame. Since we are interested in the motion, we relate the translational and rotational velocities of the next frame in terms of the previous frame. Let $u_a = [x_a \ y_a \ z_a]^T$ and $u_b = [x_b \ y_b \ z_b]^T$ denote the position of the current and next frames, respectively. Similarly, let $\varphi_a = [\alpha_a \ \beta_a \ \gamma_a]^T$ and $\varphi_b = [\alpha_b \ \beta_b \ \gamma_b]^T$ be the orientation of the current and next frames, respectively, where α, β and γ are the rotation around x, y and z axis, or pitch, yaw and roll, respectively. The 3×1 translation velocity vector of the next frame b is dependent on the translational and rotational velocities of the current frame a plus any translational velocity added to the frame b itself. This can be written as [23]

$$\dot{u}_b = R_{b,a}(\dot{u}_a + \dot{\varphi}_a \times p_b) + \dot{u}_{ob} \quad (9)$$

where $R_{b,a}$ and p_b are, respectively, the rotation matrix and position vector of the frame b relative to the frame a , and \dot{u}_{ob} is the translational velocity added to the frame b . The latter is zero if the joint associated with the frame b is not prismatic. The rotational velocity of the next frame b is dependent on the rotational velocity of the frame a plus any rotational velocity $\dot{\varphi}_{ob}$ added to the frame b itself, i.e. [23]

$$\dot{\varphi}_b = R_{b,a} \dot{\varphi}_a + \dot{\varphi}_{ob} \quad (10)$$

We start at each wheel i ($i = 1, 2, \dots, n$) contact frame which has the translational and rotational velocities $\dot{u}_i = [\dot{x}_i \ \dot{y}_i \ \dot{z}_i]^T$ and $\dot{\varphi}_i = [\dot{\alpha}_i \ \dot{\beta}_i \ \dot{\gamma}_i]^T$, and perform the frame to frame velocity propagation until we reach to the rover reference frame to obtain rover velocities $\dot{u}_r = [\dot{x}_r \ \dot{y}_r \ \dot{z}_r]^T$ and $\dot{\varphi}_r = [\dot{\alpha}_r \ \dot{\beta}_r \ \dot{\gamma}_r]^T$. Let the joint variable vector that includes each wheel-terrain contact angle, steering angle, and various prismatic and revolute joint variables be denoted by the $v_i \times 1$ vector η_i . Then we will obtain an equation of the general form

$$\begin{pmatrix} \dot{u}_r \\ \dot{\varphi}_r \end{pmatrix} = J_i \begin{pmatrix} \dot{u}_i \\ \dot{\varphi}_i \\ \dot{\eta}_i \end{pmatrix}; \quad i = 1, 2, \dots, n \quad (11)$$

where J_i is the Jacobian matrix of the wheel i . Note that the wheel translational and rotational velocity vectors \dot{u}_i and $\dot{\varphi}_i$ include various slips. For example $\dot{x}_i = r_i \dot{\theta}_i + \dot{\zeta}_{roll-i}$ where r_i is the radius of wheel i , $\dot{\theta}_i$ is the angular

velocity of that wheel, and $\dot{\zeta}_{roll-i}$ is the rolling slip rate. Similarly \dot{y}_i and \dot{z}_i can, respectively, have side slip $\dot{\zeta}_{side-i}$ and bounce $\dot{\zeta}_{bnce-i}$ (up and down off the terrain movement) components. In addition, $\dot{\alpha}_i$, $\dot{\beta}_i$ and $\dot{\gamma}_i$ can be associated, respectively, with tilt $\dot{\zeta}_{tilt-i}$, sway $\dot{\zeta}_{sway-i}$ and turn $\dot{\zeta}_{turn-i}$ slip rate components. In practice some of these slip components are unnecessary due to terrain topology and surface conditions, the path to be traversed (e.g. straight, serpentine, wavy) and mechanical arrangement of the wheels and suspension system.

Equation (11) describes the contribution of individual wheel motion and the connecting joints to the rover body motion. The net body motion is the composite effect of all wheels and can be obtained by combining (11) into a single matrix equation as

$$\begin{pmatrix} I_6 \\ \vdots \\ I_6 \end{pmatrix} \begin{pmatrix} \dot{u}_r \\ \dot{\phi}_r \end{pmatrix} = J \begin{pmatrix} \dot{u}_w \\ \dot{\phi}_w \\ \dot{\eta} \end{pmatrix} \quad (12)$$

where the composite identity matrix on the left is $6n \times n$, $\dot{u}_w = (\dot{u}_1 \ \dot{u}_2 \ \dots \ \dot{u}_n)^T$ and $\dot{u}_w = (\dot{\phi}_1 \ \dot{\phi}_2 \ \dots \ \dot{\phi}_n)^T$ are $3n \times 1$ vectors of composite wheel velocities, and $\dot{\eta}$ is the $\nu \times 1$ vector of the joint variables which has both active (actuated) and passive joints. Note that in general some wheels share common suspension links and joints so that $\nu \leq \sum_{i=1}^n \nu_i$. The composite Jacobian matrix of the rover J has a dimension of $6n \times (6n + \nu)$.

4. Example – Articulated Rover with Active Suspension (ARAS)

The articulated rover with active suspension (ARAS) to be considered here is similar to the JPL Sample Return Rover shown in Fig.4. The schematic diagram of ARAS to be analyzed is shown in Fig. 5. An articulated rover with active suspension system (ARAS) is a wheeled mobile robot consisting of a main body connected to wheels via a set of linkages and joints that can be adjusted, some actively and some passively for keeping the rover balanced. The active linkages and joints have actuators through which their values can be controlled, whereas passive ones change their values to comply with the terrain topology.

The rover has four wheels with each independently actuated and rotation angles subscripted with a clockwise direction so that θ_1, θ_4 are for the left side and θ_2, θ_3 are for the right side. At either side of the rover, two legs are connected via an adjustable hip joint. In Fig. 2 the hip angles on the left and right sides are denoted as $2\sigma_1$ and $2\sigma_2$, respectively. These joints are actuated and used for balancing the rover. The two hips are connected to the body via a differential which has an angle ρ on the left side and $-\rho$ on the right side. On a flat surface ρ is zero but becomes non-zero when one side moves up or down with respect to the other side. The differential joint ρ is passive (unactuated) and provides for the compliance with the terrain. The wheels are steerable with steering angles denoted by ψ_i . The wheel terrain contact angle δ_i is the angle between the z-axes of the i-th wheel axle frame A_i and contact coordinate frame C_i as shown in Fig. 2.

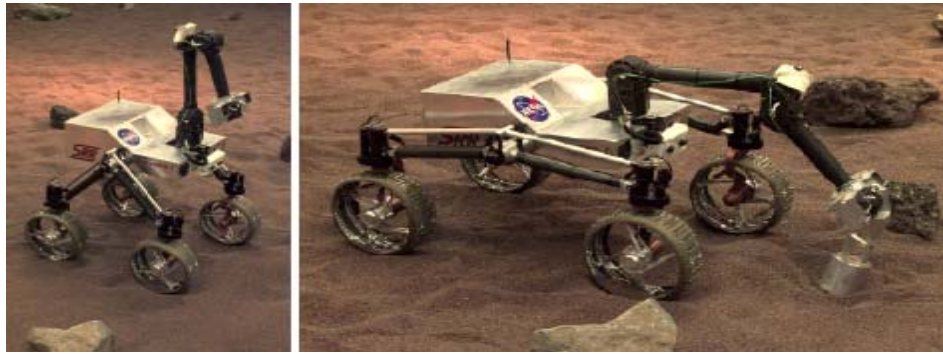


Fig. 4 The JPL's sample return rover

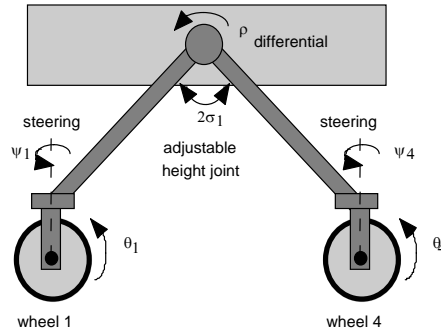


Fig. 5 Schematic diagram of the left side of ARAS

In order to derive the kinematics equations, we must assign coordinate frames. Fig. 6 illustrates our choice of coordinate frames for the left side of the rover. The right side is assigned similar frames. In Fig. 6, R is the rover reference frame whose origin is located on the center of gravity of the rover, its x-axis along the rover straight line forward motion, its y-axis across the rover body and its z-axis represents the up and down motion. The differential frame D has a vertical (along z-axis) offset denoted by k_1 and a horizontal distance of k_2 from D. The distance from the differential to the hip, denoted by k_3 , is half the width of the rover. We now introduce three more frames, all of which have origin at the wheel axle. The length of the legs from the hip to the wheel axle is k_4 . The hip frames H_1, \dots, H_4 for the four wheels are obtained from the differential frame by rotation and translation as shown with the Denavit-Hartenberg (D-H) parameters $\gamma_{dh}, d_{dh}, a_{dh}$ and α_{dh} in Table 1 and in Fig 3. Similarly the steering frames S_1, \dots, S_4 and axle frames A_1, \dots, A_4 are defined in Table 1 and Fig 2.

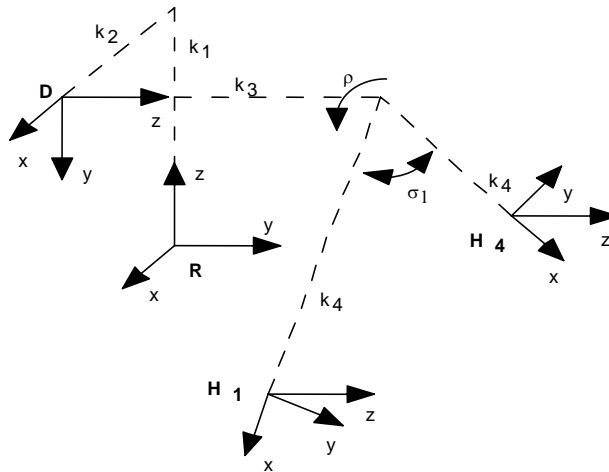


Fig. 6 Reference R, differential D, and hip H coordinate frames

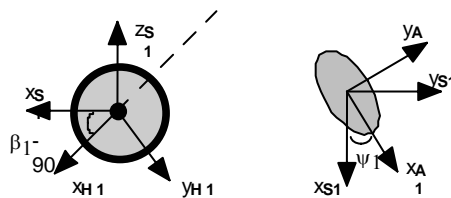


Fig. 7 Side (left figure) and top views of wheel 1

| Frame | γ_{dh} | d_{dh} | a_{dh} | α_{dh} |
|-------|------------------------|----------|----------|---------------|
| D | 0 | k_1 | k_2 | -90 |
| H1 | $90 - \sigma_1 + \rho$ | k_3 | k_4 | 0 |
| H2 | $90 - \sigma_2 - \rho$ | $-k_3$ | k_4 | 0 |
| H3 | $90 + \sigma_3 - \rho$ | $-k_3$ | k_4 | 0 |
| H4 | $90 + \sigma_4 + \rho$ | k_3 | k_4 | 0 |
| S1 | $\sigma_1 - 90$ | 0 | 0 | 90 |
| S2 | $\sigma_2 - 90$ | 0 | 0 | 90 |
| S3 | $\sigma_3 - 90$ | 0 | 0 | 90 |
| S4 | $\sigma_4 - 90$ | 0 | 0 | 90 |
| A1 | ψ_1 | 0 | 0 | 0 |
| A2 | ψ_2 | 0 | 0 | 0 |
| A3 | ψ_3 | 0 | 0 | 0 |
| A4 | ψ_4 | 0 | 0 | 0 |

Table 1 D-H Parameters for the ARAS

$k_1 = 0$ cm – vertical offset of rover reference (R) to differential (D)
 $k_2 = 0$ cm – forward offset of rover reference (R) to differential (D)
 $k_3 = 20$ cm – half the width of the rover (horizontal distance from center to wheel axle)
 $k_4 = 30$ cm – length of rover legs from hip joint to wheel axle
 $k_5 = 6.5$ cm – wheel radius

4. 1 – ARAS Jacobian Matrix using Method 1

In section 2, we defined an approach for kinematics modeling using transformation derivatives. Now we apply that methodology to ARAS. The coordinate frames in Fig. 6 were selected for consistency with D-H notation. For example, the differential frame D is obtained from the rover reference R by translating $d = k_1$ along the z-axis, translating $a = k_2$ along the x-axis, and rotating $\alpha = -90$ degrees about the x-axis. Similarly the steering frames Si and axle frames Ai are obtained using Table 1. Each coordinate frame represents one step in the kinematics chain from the rover's reference frame R to a wheel contact Ci ($i=1,\dots,4$), which can be written as

$$T_{R,Ci} = (T_{R,D})(T_{D,H1})(T_{H1,S1})(T_{S1,A1})(T_{A1,C1}), \quad i = 1, \dots, 4 \quad (13)$$

The transformations from axle frames to contact frames, $T_{Ai,Ci}$, are given by (1) rather than by D-H parameters and therefore no entries for the contact frames are provided in Table I. The other transformation matrices in (13) are obtained from Table I. Substituting these transformation matrices in (13) and simplifying, the rover reference frame to the contact transformation matrices for wheels 1, ..., 4 of the ARAS are found to be:

$$T_{R,Ci} = \begin{bmatrix} (c\alpha\psi_i c\delta_i - b_i s\alpha\delta_i) & -c\alpha\psi_i & (c\alpha\psi_i s\delta_i - b_i s\alpha\delta_i) & T_{14} \\ s\psi_i c\delta_i & c\psi_i & s\psi_i s\delta_i & T_{24} \\ (b_i s\alpha\psi_i c\delta_i - c\alpha\delta_i) & -b_i s\alpha\psi_i & (b_i s\alpha\psi_i s\delta_i + c\alpha\delta_i) & T_{34} \\ 0 & 0 & 0 & 1 \end{bmatrix}; \quad i = 1, \dots, 4 \quad (14)$$

where $b_i = \begin{cases} -1 & i = 1, 4 \\ +1 & i = 2, 3 \end{cases}$, $h_i = \begin{cases} +1 & i = 1, 2 \\ -1 & i = 3, 4 \end{cases}$ and $\begin{cases} T_{14} = k_2 + k_4 s(h_i \sigma_i + b_i \rho) - k_5 T_{13} \\ T_{24} = -b_i k_3 - k_5 T_{23} \\ T_{34} = k_1 - k_4 c(h_i \sigma_i + b_i \rho) - k_5 T_{33} \end{cases}$.

The position and orientation of the wheel at the contact points for the front wheels can be extracted from the transformation matrix (14), e.g., $x_i = T_{14}$, $y_i = T_{24}$, $z_i = T_{34}$.

Note that in the special case when the rover moves over a flat surface $\delta_i = \rho = 0$ then (14) reduces to a rotation of ψ_i about z axis, and translations $(k_2 + h_i k_4 s \sigma_i)$ along the x axis, $b_i k_3$ along the y axis, and $(k_1 - k_4 c \sigma_i)$ along the z axis. It is noted that the rover-contact transformations $T_{R,Ci}$ are functions of rover joint angles ρ , $2\sigma_1$, $2\sigma_2$, Ψ_1 , Ψ_2 , Ψ_3 , Ψ_4 and contact angle δ_i .

The rover Jacobian equations are derived from (2)-(7) using (14). This involves first forming $T_{Ci,R}^- = T_{Ci,C}^- T_{C,R}$ via (2), and (14), and taking its derivative with respect to joint angle vector $q = [\rho, 2\sigma_1, 2\sigma_2, \Psi_1, \Psi_2, \Psi_3, \Psi_4]$, contact angle δ_i , wheel rotation θ_i , and slip vector $\varepsilon = [\zeta_i, \xi_i, \eta_i]^T$ to obtain $\dot{T}_{Ci,R}^-$ as in (5). The acquired $\dot{T}_{Ci,R}^-$, and $\dot{T}_{R,R}$ given by (6) are substituted in (4), and the like elements of the matrices in both sides of (4) are equated. This gives an equation of the form (7) relating the rover position/orientation rates to the rover joint angle rates. The Jacobian matrices for wheels 1-4 are

$$\begin{bmatrix} \dot{x}_r \\ \dot{y}_r \\ \dot{z}_r \\ \dot{\alpha}_r \\ \dot{\beta}_r \\ \dot{\gamma}_r \end{bmatrix} = \begin{bmatrix} -b_i k_1 & J_{x,\sigma 1} & J_{x,\sigma 2} & J_{x,\psi} & J_{x,\theta} & J_{x,\zeta} & J_{x,\eta} & J_{x,\delta} \\ 0 & 0 & 0 & J_{y,\psi} & J_{y,\theta} & J_{y,\zeta} & J_{y,\eta} & J_{y,\delta} \\ b_i k_2 & J_{z,\sigma 1} & J_{z,\sigma 2} & J_{z,\psi} & J_{z,\theta} & J_{z,\zeta} & J_{z,\eta} & J_{z,\delta} \\ 0 & 0 & 0 & J_{\phi x,\psi} & 0 & J_{\phi x,\zeta} & 0 & J_{\phi x,\delta} \\ b_i & 0 & 0 & 0 & 0 & J_{\phi y,\zeta} & 0 & J_{\phi y,\delta} \\ 0 & 0 & 0 & J_{\phi z,\psi} & 0 & J_{\phi z,\zeta} & 0 & J_{\phi z,\delta} \end{bmatrix} \begin{bmatrix} \dot{\rho} \\ \dot{\sigma}_1 \\ \dot{\sigma}_2 \\ \dot{\psi}_i \\ \dot{\theta}_i + \dot{\xi}_i \\ \dot{\zeta}_i \\ \dot{\eta}_i \\ \dot{\delta}_i \end{bmatrix}; \quad i = 1,2,3,4 \quad (15)$$

The first column of J shows that the rocker angle contributes only to \dot{x}_r , \dot{z}_r , and pitch $\dot{\beta}_r$. The fifth and seventh columns indicate that the rolling velocity, rolling slip, and side slip have no effect on the orientation of the rover. The contributions of various rover angles to the forward rover velocity \dot{x}_r are given by the first row of the Jacobian matrix, whose elements are

$$J_{x,\sigma 1} = \begin{cases} \frac{-h_i k_4}{2} c(\sigma_i - h_i \rho) & i = 1,4; \\ 0 & i = 2,3 \end{cases}; \quad J_{x,\sigma 2} = \begin{cases} 0 & i = 1,4; \\ \frac{-h_i k_4}{2} c(\sigma_i + h_i \rho) & i = 2,3 \end{cases}; \quad J_{x,\psi} = b_i k_3 c \rho; \quad J_{x,\theta} = k_5 c \rho c \psi_i c \delta_i + b_i k_5 s \rho s \delta_i;$$

$$\begin{aligned} J_{x,\zeta} &= -k_1 s \psi_i s \delta_i - b_i k_3 c \rho c \delta_i - k_3 s \rho c \psi_i s \delta_i + k_4 c(\sigma_i + b_i h_i \rho) s \psi_i s \delta_i; \\ J_{x,\eta} &= -c \rho s \psi_i; \quad J_{x,\delta} = k_1 c \psi_i - k_3 s \rho s \psi_i - k_4 c(\sigma_i + b_i h_i \rho) c \psi_i; \\ J_{y,\psi} &= k_2 c \rho + b_i k_1 s \rho + h_i k_4 s \sigma_i; \quad J_{y,\theta} = k_5 s \psi_i c \delta_i; \\ J_{y,\zeta} &= -b_i k_1 s \rho c \delta_i + k_1 c \rho c \psi_i s \delta_i - k_2 c \rho c \delta_i - b_i k_2 s \rho c \psi_i s \delta_i - h_i k_4 s \sigma_i c \delta_i - k_4 c \sigma_i c \psi_i s \delta_i; \\ J_{y,\eta} &= c \psi_i; \quad J_{y,\delta} = k_1 c \rho s \psi_i - b_i k_2 s \rho s \psi_i - k_4 c \sigma_i s \psi_i. \end{aligned}$$

The contributions of various angles to the vertical motion of the rover, which are given by the third row, are

$$J_{z,\sigma 1} = \begin{cases} \frac{-k_4}{2} s(\sigma_i - h_i \rho) & i = 1,4; \\ 0 & i = 2,3 \end{cases}; \quad J_{z,\sigma 2} = \begin{cases} 0 & i = 1,4; \\ \frac{-k_4}{2} s(\sigma_i + h_i \rho) & i = 2,3 \end{cases}$$

$$\begin{aligned} J_{z,\psi} &= k_3 s \rho \\ J_{z,\theta} &= b_i k_5 s \rho c \psi_i c \delta_i - k_5 c \rho s \delta_i \\ J_{z,\zeta} &= k_2 s \psi_i s \delta_i - k_3 s \rho c \delta_i + b_i k_3 c \rho c \psi_i s \delta_i + h_i k_4 s(\sigma_i + b_i h_i \rho) s \psi_i s \delta_i \\ J_{z,\eta} &= -b_i s \rho s \psi_i \end{aligned}$$

$$J_{z,\delta} = -k_2 c \psi_i + b_i k_3 c \rho s \psi_i - h_i k_4 s (\sigma_i + b_i h_i \rho) c \psi_i$$

The last three rows determine the contributions of rover joints to the orientation of the rover and are given by

$$\begin{aligned} J_{\alpha,\psi} &= b_i s \rho; & J_{\alpha,\zeta} &= -b_i s \rho c \delta_i + c \rho c \psi_i s \delta_i; & J_{\alpha,\delta} &= c \rho s \psi_i; & J_{\beta,\zeta} &= s \psi_i s \delta_i; & J_{\beta,\delta} &= -c \psi_i; & J_{\gamma,\psi} &= -c \rho; \\ J_{\gamma,\zeta} &= c \rho c \delta_i + b_i s \rho c \psi_i s \delta_i; & J_{\gamma,\delta} &= b_i s \rho s \psi_i. \end{aligned}$$

4. 2 – ARAS Jacobian Matrix using Method 2

The second methodology, which is defined in section 3, is based on the propagation of position and orientation velocities through wheels and various joints and linkages of the rover. In order to compare the performance of our two methodologies for kinematics modeling of articulated rovers, here we implement this approach also to the JLP Sample Return Rover.

We must now use the basic frame to frame equations (9)-(10) and go through the frames sequentially from wheel i terrain contact C_i , wheel axle A_i , steering S_i , hip H_i , differential D, and finally to the rover reference R. Equation (9)-(10) for the contact to the axle becomes

$$\begin{aligned} \dot{u}_{A_i} &= R_{A_i,C_i} \left(\dot{u}_{C_i} + \dot{\phi}_{C_i} \times (0 \ 0 \ r)^T \right) \\ \dot{\phi}_{A_i} &= R_{A_i,C_i} \dot{\phi}_{C_i} + (0 \ -\dot{\delta}_i \ 0)^T \end{aligned} \quad (16)$$

where the rotation matrix is $R_{A_i,C_i} = \begin{pmatrix} c \delta_i & 0 & s \delta_i \\ 0 & 1 & 0 \\ -s \delta_i & 0 & c \delta_i \end{pmatrix}$, as evident from Fig. 2. Note that wheel velocities at the terrain contact are denoted in (11) as $\dot{u}_{C_i} \equiv \dot{u}_i$ and $\dot{\phi}_{C_i} \equiv \dot{\phi}_i$. Next we form wheel i axle to steering velocity propagation as

$$\begin{aligned} \dot{u}_{S_i} &= R_{S_i,A_i} \left(\dot{u}_{A_i} + \dot{\phi}_{A_i} \times (0 \ 0 \ 0)^T \right) \\ \dot{\phi}_{S_i} &= R_{S_i,A_i} \dot{\phi}_{A_i} + (0 \ 0 \ -\dot{\psi}_i)^T \end{aligned} \quad (17)$$

where $R_{S_i,A_i} = \begin{pmatrix} c \psi_i & -s \psi_i & 0 \\ s \psi_i & c \psi_i & 0 \\ 0 & 0 & 1 \end{pmatrix}$. The next in the chain is the hip frame, and we can write

$$\begin{aligned} \dot{u}_{H_i} &= R_{H_i,S_i} \left(\dot{u}_{S_i} + \dot{\phi}_{S_i} \times (0 \ 0 \ 0)^T \right) \\ \dot{\phi}_{H_i} &= R_{H_i,S_i} \dot{\phi}_{S_i} + (0 \ 0 \ -h_i \dot{\sigma}_i)^T \end{aligned} \quad (18)$$

with $R_{H_i,S_i} = \begin{pmatrix} s(h_i \sigma_i) & 0 & -c(h_i \sigma_i) \\ -c(h_i \sigma_i) & 0 & s(h_i \sigma_i) \\ 0 & 1 & 0 \end{pmatrix}$, $\sigma_4 = \sigma_1$, $\sigma_3 = \sigma_2$, and $h_i = \begin{cases} 1 & i = 1,2 \\ -1 & i = 3,4 \end{cases}$. The differential frame velocities are obtained from (9)-(10) and Table 1 as

$$\begin{aligned} \dot{u}_{D_i} &= R_{D_i,H_i} \left(\dot{u}_{H_i} + \dot{\phi}_{H_i} \times (-k_4 \ 0 \ b_i k_3)^T \right) \\ \dot{\phi}_{D_i} &= R_{D_i,H_i} \dot{\phi}_{H_i} + (0 \ 0 \ h_i \dot{\sigma}_i + b_i \dot{\rho}_i)^T \end{aligned} \quad (19)$$

$$\text{where } R_{Di,Hi} = \begin{pmatrix} s(h_i\sigma_i + b_i\rho_i) & -c(h_i\sigma_i + b_i\rho_i) & 0 \\ c(h_i\sigma_i + b_i\rho_i) & s(h_i\sigma_i + b_i\rho_i) & 0 \\ 0 & 0 & 1 \end{pmatrix}, \quad \rho_4 = \rho_1 = \rho, \rho_2 = \rho_3 = -\rho, \quad \text{and}$$

$$b_i = \begin{cases} -1 & i = 1,4 \\ 1 & i = 2,3 \end{cases}. \quad \text{Finally, the rover velocities are obtained as}$$

$$\begin{aligned} \dot{u}_r &= R_{r,Di} \left(\dot{u}_{Di} + \dot{\phi}_{Di} \times (-k_2 \quad -k_1 \quad 0)^T \right) \\ \dot{\phi}_r &= R_{r,Di} \dot{\phi}_{Di} + (0 \quad 0 \quad 0)^T \end{aligned} \quad (20)$$

Substituting recursively (16) through (19) into (20) we obtain an equation of the form (11) where $\dot{\eta}_i = (\dot{\rho}_i \quad \dot{\sigma}_i \quad \dot{\psi}_i \quad \dot{\delta}_i)^T$. The Jacobian matrices J_i and their elements are found as

$$\begin{bmatrix} \dot{x}_r \\ \dot{y}_r \\ \dot{z}_r \\ \dot{\alpha}_r \\ \dot{\beta}_r \\ \dot{\gamma}_r \end{bmatrix} = \begin{bmatrix} J_{1,1} & J_{1,2} & J_{1,3} & J_{1,4} & J_{1,5} & J_{1,6} & -b_1k_1 & J_{1,8} & J_{1,9} & J_{1,10} \\ J_{2,1} & c\psi_i & J_{2,3} & J_{2,4} & J_{2,5} & J_{2,6} & 0 & 0 & J_{2,9} & J_{2,10} \\ J_{3,1} & J_{3,2} & J_{3,1} & J_{3,4} & J_{3,5} & J_{3,6} & b_1k_2 & J_{3,8} & J_{3,9} & J_{3,10} \\ 0 & 0 & 0 & J_{4,4} & J_{4,5} & J_{4,6} & 0 & 0 & J_{4,9} & J_{4,10} \\ 0 & 0 & 0 & J_{5,4} & c\psi_i & J_{5,6} & b_i & 0 & 0 & -c\psi_i \\ 0 & 0 & 0 & J_{6,4} & J_{6,5} & J_{6,6} & 0 & 0 & -c\rho & J_{6,10} \end{bmatrix} \begin{bmatrix} \dot{x}_i \\ \dot{y}_i \\ \dot{z}_i \\ \dot{\alpha}_i \\ \dot{\beta}_i \\ \dot{\gamma}_i \\ \dot{\rho} \\ \dot{\sigma}_i \\ \dot{\psi}_i \\ \dot{\delta}_i \end{bmatrix}; \quad i=1, 2, 3, 4 \quad (21)$$

The first row defines contributions of various angles to the forward rover velocity \dot{x}_r , as follows

$$\begin{aligned} J_{1,1} &= b_1s\rho s\delta_i + c\rho c\psi_i c\delta_i; & J_{1,2} &= -c\rho s\psi_i; & J_{1,3} &= -b_1s\rho c\delta_i + c\rho c\psi_i s\delta_i \\ J_{1,4} &= -k_1s\psi_i c\delta_i - k_3s\rho c\psi_i c\delta_i + b_1k_3c\rho s\delta_i + k_4c(\sigma_i + b_1h_i\rho)s\psi_i c\delta_i + k_5c\rho s\psi_i \\ J_{1,5} &= -k_1c\psi_i + k_3s\rho s\psi_i + k_4c(\sigma_i + b_1h_i\rho)c\psi_i + k_5c\rho c\psi_i c\delta_i + b_1k_5s\rho s\delta_i \\ J_{1,6} &= -k_1s\psi_i s\delta_i - k_3s\rho c\psi_i s\delta_i - b_1k_3c\rho c\delta_i + k_4c(\sigma_i + b_1h_i\rho)s\psi_i s\delta_i \\ J_{1,8} &= -\frac{h_1k_4}{2}c(\sigma_i + b_1h_i\rho); & J_{1,9} &= b_1k_3c\rho; & J_{1,10} &= k_1c\psi_i - k_3s\rho s\psi_i - k_4c(\sigma_i + b_1h_i\rho)c\psi_i \end{aligned}$$

The second row defines contributions of various angles to the side motion of the rover as follows:

$$\begin{aligned} J_{2,1} &= s\psi_i c\delta_i; & J_{2,1} &= s\psi_i c\delta_i \\ J_{2,4} &= k_1c\rho c\psi_i c\delta_i + b_1k_1s\rho s\delta_i + k_2c\rho s\delta_i - b_1k_2s\rho c\psi_i c\delta_i - k_4c\sigma_i c\psi_i c\delta_i - k_5c\psi_i \\ J_{2,5} &= -k_1c\rho s\psi_i + b_1k_2s\rho s\psi_i + k_4c\sigma_i s\psi_i + k_5s\psi_i c\delta_i \\ J_{2,6} &= k_1c\rho c\psi_i s\delta_i - b_1k_1s\rho c\delta_i - k_2c\rho c\delta_i - b_1k_2s\rho c\psi_i s\delta_i - k_4c\sigma_i c\psi_i s\delta_i - h_1k_4s\sigma_i c\delta_i \\ J_{2,9} &= b_1k_1s\rho + k_2c\rho + h_1k_4s\sigma_i; & J_{2,10} &= k_1c\rho s\psi_i - b_1k_2s\rho s\psi_i - k_4c\sigma_i s\psi_i \end{aligned}$$

The contributions of various angles to the vertical motion of the rover, which are given by the third row, are

$$\begin{aligned} J_{3,1} &= b_1s\rho c\psi_i c\delta_i - c\rho s\delta_i; & J_{3,2} &= -b_1s\rho s\psi_i; & J_{3,3} &= b_1s\rho c\psi_i s\delta_i + c\rho c\delta_i; \\ J_{3,4} &= k_2s\psi_i c\delta_i + k_3s\rho s\delta_i + b_1k_3c\rho c\psi_i c\delta_i + h_1k_4s(\sigma_i + b_1h_i\rho)s\psi_i c\delta_i + b_1k_5s\rho s\psi_i; \\ J_{3,5} &= k_2c\psi_i - b_1k_3c\rho s\psi_i + h_1k_4s(\sigma_i + b_1h_i\rho)c\psi_i - k_5c\rho s\delta_i + b_1k_5s\rho c\psi_i c\delta_i; \\ J_{3,6} &= k_2s\psi_i s\delta_i - k_3s\rho c\delta_i + b_1k_3c\rho c\psi_i s\delta_i + h_1k_4s(\sigma_i + b_1h_i\rho)s\psi_i s\delta_i; \end{aligned}$$

$$J_{3,8} = -\frac{k_4}{2}s(\sigma_i + b_i h_i \rho) ; \quad J_{3,9} = k_3 s \rho ; \quad J_{3,10} = -k_2 c \psi_i + b_i k_3 c \rho s \psi_i - h_i k_4 s(\sigma_i + b_i h_i \rho) c \psi_i$$

The last three rows determine the contributions of rover joints to the orientation of the rover and are given by

$$\begin{aligned} J_{4,4} &= b_i s \rho s \delta_i + c \rho c \psi_i c \delta_i ; & J_{4,5} &= -b_i s \rho s \psi_i ; & J_{4,6} &= -b_i s \rho c \delta_i + c \rho c \psi_i s \delta_i ; & J_{4,9} &= b_i s \rho \\ J_{4,10} &= c \rho s \psi_i ; & J_{5,4} &= s \psi_i c \delta_i ; & J_{5,6} &= s \psi_i s \delta_i ; & J_{6,4} &= b_i s \rho c \psi_i c \delta_i - c \rho s \delta_i ; \\ J_{6,5} &= -b_i s \rho s \psi_i ; & J_{6,6} &= b_i s \rho c \psi_i s \delta_i + c \rho c \delta_i ; & J_{6,10} &= b_i s \rho s \psi_i \end{aligned}$$

4.3 – Matlab Implementation

Both methods were implemented in Matlab using the Symbolic Math Toolbox. For method 1, we make use of two scripts to compute elements of equations (14) and (15) respectively. Let us call them Transform-Matrix and Jacobian-Matrix. The Transform-Matrix script computes the homogeneous transform matrix T_{R,C_i} for all wheels of ARAS. In order to accomplish this, it finds transformation matrices between every coordinate frame in the kinematics chain and then multiplies them according to equation (13). This script uses the information provided in Table I to compute the first four transformations in equation (13). Also, it uses equation (1) to find transformation matrix from axle frame A_i to contact frame C_i .

The Jacobian-Matrix script first calls Transform-Matrix script and then computes transformation matrix T_{C_i, \bar{C}_i} , which goes from contact frame C_i to motion frame \bar{C}_i . The transformation matrix from rover reference frame to motion frame T_{R, \bar{C}_i} comes as a result of multiplying T_{R,C_i} and T_{C_i, \bar{C}_i} . Next, $T_{\bar{C}_i, R}$ is found and partial derivatives of it are computed according to (5). After that, the script evaluates matrix products resulting from multiplying right side elements of equation (4). Finally, the Jacobian matrix is formed by equating the like matrix elements on both sides and extracting the rover configuration rate vector \dot{u} . Therefore, basically this script is providing a description of the contribution of individual wheel motion and the connecting joints to the rover body motion.

As we can see, there are several rotations and translations that need to be applied during the process of finding transformation matrices. Thus, we created functions Rot() and Trans(), which are called from both of the above scripts, to compute homogeneous transformations matrices for pure rotation and translation. The function Rot() uses elementary rotations as follows:

$$rot(e_1, \varphi) = \begin{bmatrix} 1 & 0 & 0 \\ 0 & c\varphi & -s\varphi \\ 0 & s\varphi & c\varphi \end{bmatrix} \quad \text{Rotation about x-axis}$$

$$rot(e_2, \varphi) = \begin{bmatrix} c\varphi & 0 & s\varphi \\ 0 & 1 & 0 \\ -s\varphi & 0 & c\varphi \end{bmatrix} \quad \text{Rotation about y-axis}$$

$$rot(e_3, \varphi) = \begin{bmatrix} c\varphi & -s\varphi & 0 \\ s\varphi & c\varphi & 0 \\ 0 & 0 & 1 \end{bmatrix} \quad \text{Rotation about z-axis}$$

On the other hand, method 2 computes position and orientation velocity propagation from frame to frame using a recursive function, which is called by a script. According to the information given in Table 1, this script fills a matrix with the D-H parameters table of the ARAS. Each row in this matrix represents rotational and translational transformations from frame to frame. Also, one more row is added to the matrix for a translation along z-axis of k_5 and a rotation about y-axis of δ_i . This corresponds to the transformation matrix from the axle frame A_i to the contact frame C_i , which is expressed in (1).

The function receives as parameter an index number indicating which row of the matrix needs to be consulted at each step of the process. Then it uses (9) and (10) recursively to find the propagation of position and orientation

velocities from frame to frame starting at each wheel contact frame C_i . Finally, the output of this function is a 6x1 vector that contains position and orientation rover velocities, i.e. $[\dot{x}_r \ \dot{y}_r \ \dot{z}_r \ \dot{\alpha}_r \ \dot{\beta}_r \ \dot{\gamma}_r]^T$. In this vector, we find the contribution of various angle rates to the velocity of the rover. The Jacobian matrix is formed using elements from each row of the vector. Columns of the matrix are arranged in this order:

$$\dot{x}_i \ \dot{y}_i \ \dot{z}_i \ \dot{\alpha}_i \ \dot{\beta}_i \ \dot{\gamma}_i \ \dot{\rho} \ \dot{\sigma}_i \ \dot{\psi}_i \ \dot{\delta}_i .$$

It is noted that Matlab does not provide the simplest form expression for the elements of the Jacobian matrices. Therefore, the equations must be simplified by using the trigonometric and algebraic identities.

5 – Conclusions

Two approaches for kinematics modeling of articulated rovers have been presented. These methodologies have been applied to an articulated rover with active suspension. The first methodology derives the equations of motion of the rover components relative to the rover reference frame while the second simply uses a recursive algorithm to compute position-orientation velocity propagation through wheels and various joint linkages of the rover. As we have seen, under the same assumptions, results are same in both cases. Note that columns 1,4,5,7, and 8 of equation (15) correspond to columns 7,9,1,2, and 10, respectively, in equation (21). Also, columns 2 and 3 in equation (15) correspond to column 8 in equation (21). Even though the two methods produce identical results, the second approach is easier to implement since it works recursively and no extractions are needed. Thus, it eliminates the necessity of equating like matrix elements and extracting terms. In addition, because in the second method we deal directly with position and orientation velocities, we do not have to compute partial derivatives.

6 – References

- [1] P. Schenker, T. Huntsberger, P. Pirjanian, E. Baumgartner, and E. Tunstel, “ Planetary rover developments supporting Mars exploration, sample return and future human robotic colonization,” *Autonomous Robots*, vol. 14, pp. 103-126, 2003.
- [2] R. Volpe, “Rover functional autonomy development for Mars mobile science,” *Proc. IEEE Aerospace Conf.* pp. 643-652, 2003.
- [3] Y. Gonthier., and E. Papadopoulos, “ On the development of a real-time simulator for an electro-hydraulic forestry machine. *Proc. IEEE Int. Conf. Robotics & Automation*, Leuven, Belgium, 1998.
- [4] A-J. Baerveldt Ed., “Agricultural Robotics”, *Autonomous Robots*, Vol 13-1, Kluwer Academic Publishers, 2002.
- [5] J. Cunningham, J. Roberts, P. Corke and H. Durrant-Whyte, “Automation of underground LHD and truck haulage,” *Proc. Australian IMM Conf.* pp. 241-246, 1998.
- [6] Ch. DeBolt, Ch. O'Donnell, S. Freed, and T. Nguyen, “The bugs ‘basic uxo gathering system’ project for uxo clearance and mine countermeasures. *Proc. IEEE Int. Conf. Robotics and Automation*, pp. 329-334, Albuquerque, N.M., 1997.
- [7] K. Iagnemma, and S. Dubowski, “Traction Control of wheel mobile robots in rough terrain with applications to planetary rovers,” *Int. J. Robotics Res.*, vol. 23, No. 10-11, pp. 1029-1040, 2003.
- [8] I. J. Cox and G.T. Wilfong, *Autonomous Robot Vehicles*, Springer-Verlag, N.Y. 1990.
- [9] K. Iagnemma, F. Genot and S. Dubowski, “Rapid physics-based rough terrain rover planning with sensor and control uncertainty,” *Proc. IEEE Int. Robotics and Automation*, pp. 2286-2291, Detroit, MI, 1999.
- [10] P.F. Muir and C.P. Neumann, “Kinematic modeling of wheeled mobile robots,” *J. Robotics Systems*, vol. 4, no. 2, pp. 282-340, 1987.
- [11] J.C. Alexander and J.H. Maddocks, “On the kinematics of wheeled mobile robots,” *Int. J. Robotics Research*, vol. 8, no. 5, pp. 15-26, 1989.
- [12] G. Campion, G. Bastin and diAndrea-Novel, “Structural properties and classification of kinematic and dynamic models for wheel mobile robots,” *IEEE Trans. Robotics and Automation*, Vol. 12, No. 1, Feb. 1996.
- [13] J. Borenstein, “Control and kinematics design of multi-degree of freedom robots with compliant linkage,” *IEEE Trans. Robotics and Automation*, pp. 21-35, 1995.
- [14] R. Rajagopalan, “A generic kinematic formulation for wheeled mobile robots,” *J. Robotics Systems*, vol. 14, no. 2, pp. 77-91, 1997.
- [15] B-J. Yi and W.K. Kim, “The kinematics for redundancy actuated omnidirectional mobile robots,” *J. Robotics Systems*, vol. 19, no. 6, pp. 255-267, 2002.

- [16] R. L. Williams, B. E. Carter, P. Gallina and G. Rosati, "Dynamic model with slip for wheeled omnidirectional robots," IEEE Trans. Robotics and Automation, Vol. 18, No. 3, pp. 285-293, 2002.
- [17] M. Tarokh, G. McDermott, S. Hayati, and J. Hung, "Kinematic modeling of a high mobility Mars rover," Proc. IEEE Int. Conf. Robotics and Automation, pp. 992-998, Detroit, MI, 1999.
- [18] K. Iagnemma and S. Dubowski, "Vehicle-ground contact angle estimation with application to mobile robot traction," Proc. 7th Int. Conf. on Advances on Robot Kinematics, Ark '00, pp. 137-146, 2000.
- [19] J. Balam, "Kinematic observers for articulated rovers," Proc. IEEE Int. Conference on Robotics and Automation, pp. 2597-2604, San Francisco, CA, 2000.
- [20] S. Sreenivasan, and K. Waldron (1996). Displacement analysis of an actively articulated vehicle configuration with extensions to motion planning on uneven terrain. *Trans. ASME J. Mechanical Design*, vol. 118, pp. 312-317, 1996.
- [21] T. Tarokh, and G. McDermott, "Kinematics modeling and analysis of articulated rovers," *IEEE Trans. Robotics*, vol. 21, No. 4, 539-553.
- [22] G. McDermott, M. Tarokh and L. Mireles has been submitted to 7th IFAC Int. Conference on Robot Control, to be held in Italy, September 2006.
- [23] J. J. Craig, Introduction to Robotics, 2nd Ed, Adelson-Wesley Publishing, 1989.